Molecular Simulation of the High-Pressure Phase Equilibrium of the System Carbon Dioxide−Methanol−Water

Tamás Kristóf,*,† Johannes Vorholz,‡,§ and Gerd Maurer‡

Department of Physical Chemistry, University of Veszprém, H-8201 Veszprém, P.O. Box 158, Hungary, and Lehrstuhl für Technische Thermodynamik, Universität Kaiserslautern, D-67653 Kaiserslautern, Germany

Received: February 26, 2002; In Final Form: May 13, 2002

The high-pressure phase equilibrium of the system carbon dioxide−methanol−water was studied by molecular simulation at temperatures near the critical temperature of carbon dioxide. The system was modeled by multisite Lennard-Jones plus Coulomb intermolecular potentials with common combining rules for unlike site interactions. Good agreement was observed between experimental and simulated phase equilibrium data. Reasonably accurate predictions were obtained for the two-phase liquid−liquid and three-phase liquid−liquid−vapor coexistences.

1. Introduction

The high-pressure multiphase behavior of binary and ternary mixtures, where at least one component is a gas, has attracted considerable attention in recent years. Mixtures of water and a hydrophilic organic solvent, e.g., an alcohol, a ketone, or a carboxylic acid, exhibit complex phase behavior when pressurized with carbon dioxide at temperatures near its critical temperature. Although water and the organic solvent are completely miscible at ambient conditions, by pressurization with carbon dioxide a liquid−liquid phase separation is observed resulting in a ternary liquid−liquid−vapor coexistence. Such equilibria are traditionally modeled by means of semiempirical equations of state (EoS) applying mixing rules with adjustable parameters, which have to be fitted to experimental data.

Parallel to the development of simulation methodology and the increasing performance of computers, molecular simulation is becoming a more and more attractive tool for the prediction of fluid properties. Because of its well-established basis of statistical mechanics, molecular simulation may provide, in the future, better predictive capabilities than classical thermodynamic models as well as a better understanding of the relationship between molecular level properties and the thermodynamic behavior of substances. Due to the evolution of molecular simulation methods, simulations applying relatively complex intermolecular interaction models have become possible. However, to get reliable statistical averages for the thermodynamic properties within reasonable computing time, simplified intermolecular interaction models, so-called "effective pair potentials", are predominantly used in simulations.

The aim of this work is to investigate the high-pressure phase equilibria of the ternary system carbon dioxide−methanol−water by molecular simulation using as input molecular-based effective pair potentials for the pure components from the literature. As is shown in Figure 1, this system exhibits a liquid−liquid−vapor (L_1L_2V) three-phase region (Efremova and Shvarts;[1] Yoon et al.[2]) at temperatures higher than, but not far from, the critical temperature of carbon dioxide. Although only a few experimental data points are available, the region of ternary three-phase equilibrium of the system has been located within a small pressure range (not much wider than 0.5 MPa) between a lower critical endpoint line and an upper critical endpoint line. At the lower critical endpoint line the liquid phases become critical and coexist with a vapor phase. At the upper critical endpoint line the carbon dioxide rich liquid becomes critical with the vapor and the critical phases coexist with a water-rich liquid. The pressure region in which a three-phase equilibrium is observed decreases with increasing temperature. The three-phase equilibrium disappears at a tricritical point (T_{TCP} = 317.8 K, p_{TCP} = 8.92 MPa[1]), where all three phases become critical.

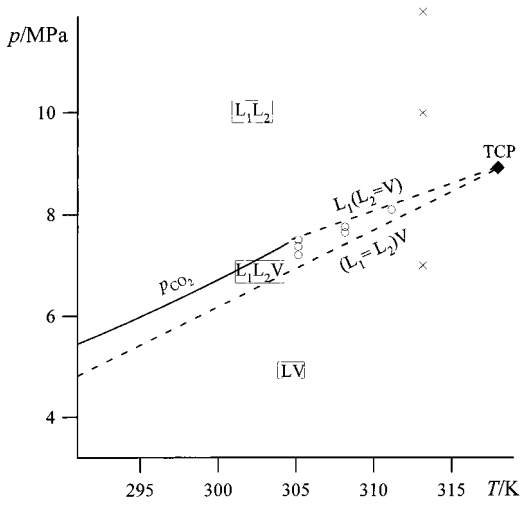

Figure 1. Qualitative pressure−temperature diagram. (L_1=L_2)V and L_1(L_2=V) indicate the lower and upper critical endpoint lines of the three-phase region, respectively; p_{CO_2} denotes the correct vapor pressure curve of carbon dioxide. ○, experimental three-phase coexistence points;[2] ◆, tricritical point (TCP) ;[1] ×, state points of two-phase equilibrium investigated experimentally;[2] L_1L_2, liquid−liquid two-phase region; LV, vapor−liquid two-phase region; L_1L_2V, three-phase region.

In the present work the Gibbs ensemble Monte Carlo (GEMC) simulation method[3] for the direct simulations of fluid-phase equilibria was applied to investigate the two-phase as well as

* Corresponding author. E-mail: kristoft@almos.vein.hu.
† University of Veszprém.
‡ Universität Kaiserslautern.
§ Present address: DEGUSSA AG, Rodenbacher Chaussee 4, D-63457 Hanau-Wolfgang, Germany.

10.1021/jp020532x CCC: $22.00 © 2002 American Chemical Society
Published on Web 06/29/2002

the three-phase equilibrium. Two-phase simulations[3,4] were also performed using the semi-grand canonical scheme.[5,6] Three-phase molecular simulations were performed according to a proposal by Canongia Lopes and Tildesley.[7] The intermolecular interactions were approximated by site−site effective pair potentials. To the knowledge of the authors, such high-pressure molecular simulation studies of two-phase as well as three-phase equilibria have not been reported in the literature. A recent publication of Lísal et al.[8] illustrates the possibility to attain accurate predictions for binary vapor−liquid equilibria with newly developed site−site effective pair potentials utilizing the Reaction GEMC technique.[9] Moreover, the two-phase GEMC results for the system methanol−ethane at 298.15 K gave some indication that the model system exhibits liquid−liquid−vapor equilibria at high pressures close to the pressure of the experimental three-phase line of the real system. A direct simulation of such three-phase equilibria appears to be straightforward when using the multiphase GEMC approach.[7] However, reliable results by this method (ensemble averages) can only be obtained for the coexisting phases if the energy barriers, which separate the different phases, are sufficiently high.

2. Methods and Computational Details

The interactions between molecules were represented by site−site potential models consisting of Lennard-Jones (6−12) and Coulomb potentials. The EPM2 model of Harris and Yung for carbon dioxide[10] and the model proposed by van Leeuwen and Smit[11] for methanol were applied in all calculations. These models reproduce well the vapor−liquid equilibrium of the pure substances. The potential models, which thus far have only been developed for water, yield coexistence properties albeit in poorer agreement with experimental data. However, in the temperature range of interest in the present work, the SPC[12] and the TIP4P[13] models provide satisfactory agreement with experimental results.

The simulated systems included 450, 512, 600, or in some cases (during the three-phase GEMC simulations) up to 800 particles (N). The runs were started from a face-centered cubic lattice configuration, a random distribution, or an output configuration of a previous run. The equilibration period in the simulations varied between 10 000 and 30 000 cycles, and the total length of the runs included up to 80 000 cycles. Each cycle consisted of N (=450, 512, 600, or 800) attempted particle displacements in the subsystems, a volume change of the subsystems, and, depending on the system densities, between 50 and 6000 attempted particle transfers (such that two to four successful particle transfers per cycle were obtained). The particle for the displacement (translation and rotation) or transfer step was selected randomly; the type of move was selected randomly but with a fixed probability. The maximum changes (displacement of a selected molecule and volume change) were adjusted to obtain, where possible, a 35−50% acceptance rate for the attempted move. The selection probability of the species to be transferred was adjusted such that approximately the same number of successful transfers was achieved for each species. Furthermore, configurational bias techniques[14−17] and particle identity exchanges[18] were employed in order to increase the sampling efficiency for the transfer step at high densities.

Parallel to the two-phase GEMC, three-phase GEMC simulations[7] were also carried out in the expected range of three-phase high-pressure coexistence. The procedure was similar to that of the two-phase simulations, the only difference being the need for selecting the pairs of subsystems for the exchange steps: this selection was made randomly with equal probabilities. Note that three-phase equilibria in ternary mixtures can be obtained by carrying out simulations in three separate boxes and fixing up to two intensive variables, e.g., pressure and temperature.

In several cases, the two-phase GEMC simulations, applied mainly at constant pressure and temperature (NpT-GEMC),[4] were combined with the semi-grand canonical scheme.[5,6] Here, the direct particle transfer move that ensures the chemical equilibrium of the given component was applied only for the carbon dioxide molecules, as their transfer has a relatively high acceptance rate in the present system. The exchange of the identity of carbon dioxide and methanol molecules in one subsystem with a simultaneous reverse exchange of the identity in the other subsystem represents a further type of particle transfer move. (This indirect transfer step together with the direct transfer step equilibrates the chemical potential of methanol.) To ensure also the chemical equilibrium for the third component (water), identity exchange moves with pairs of methanol and water molecules were performed independently, but governed by the same preset chemical potential difference (i.e., the difference between the chemical potentials of methanol and water), in each of the subsystems. Because of this semi-grand canonical move, the total system becomes open for methanol and water.

Utilizing a further type of open two-phase GEMC calculation, where molecular exchanges for carbon dioxide between the phases and a reservoir with a specified chemical potential were performed,[19] several results concerning the two-phase coexistence of the system were cross-checked. These results are not shown here.

Two different methods were used for handling the long-range interactions. In one case, the potential energy functions were truncated at a spherical cutoff distance equal to half the box length of the respective simulation cell. The long-range corrections for the Lennard-Jones interactions were estimated by assuming that the pair correlation functions have approximately unit values beyond the cutoff radius[20] and the long-range Coulomb interactions were treated using the reaction field method.[20,21] In the other case, the Lennard-Jones part of the intermolecular energy was calculated with a method proposed by Theodorou and Suter[22] and the contribution of the Coulomb interactions was estimated via Ewald sums.[20,23] Under the conditions studied, the two methods lead to nearly identical results. The Lennard-Jones parameters for interactions between unlike groups were calculated either by applying the conventional Lorentz−Berthelot combining rules or the geometric mean rule for both, core diameter and energy well depth; i.e., no adjustable binary interaction parameters were introduced. The influence of the different combining rules is discussed in the following section.

In the course of the simulations the convergence profiles of the thermodynamic quantities of interest were monitored. Estimates for the error bars were made by dividing the whole runs into 20−50 blocks and calculating the standard deviation of the block averages.[20]

3. Results and Discussion

At selected temperatures and pressures the two-phase coexistences of the system were determined by two-phase NpT-GEMC simulations using the SPC water model. The simulation results are compared with experimental vapor−liquid or liquid−liquid equilibrium data from Yoon et al.[2] as well as with results from the Peng−Robinson equation of state (PR-EoS) applying the Huron−Vidal mixing rule with interaction parameters from binary data alone (cf. Adrian et al.[24]). The results of the

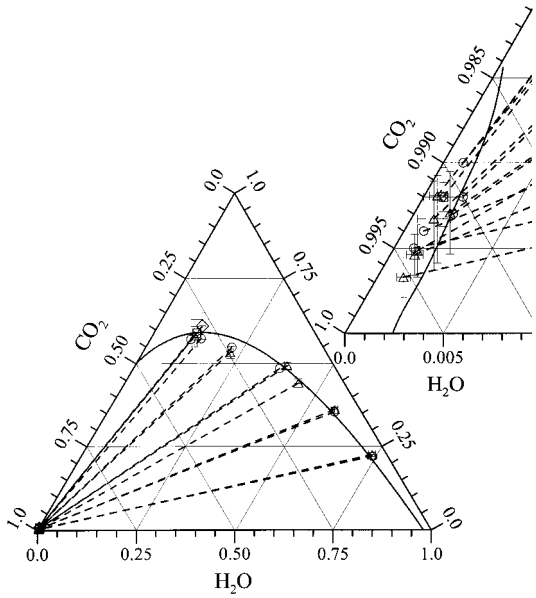

Figure 2. Liquid−vapor equilibrium mole fractions at 313.15 K and 7.0 MPa. ○, experimental results;[2] △, □, ◇ (see text), two-phase Gibbs ensemble simulations (error bars indicate statistical uncertainties). Coexisting state points are connected by dashed lines. The solid lines denote results from the PR-EoS.[24]

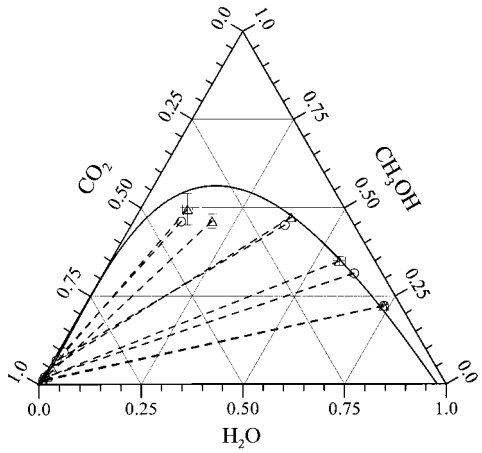

Figure 3. Liquid−liquid equilibrium mole fractions at 313.15 K and 10.0 MPa. ○, experimental results;[2] △, two-phase Gibbs ensemble simulations (error bars indicate statistical uncertainties). Coexisting state points are connected by dashed lines. The solid line denotes results from the PR-EoS[24] for the boundary of the two-phase region.

molecular simulation are summarized in Tables 1−3. Figures 2−4 show the equilibrium results for the mole fractions (x) at 313.15 K, where experimental results for the two-phase coexistence are available. Figure 2 shows the comparison between experimentally determined and calculated (i.e., from the PR-EoS as well as from molecular simulation) mole fractions for 7 MPa, i.e., at a pressure below the critical pressure of carbon dioxide. Figures 3 and 4 show a similar comparison for 10 and 12 MPa, where liquid−liquid equilibrium is expected[24] (cf. Figure 1). The ternary diagrams demonstrate the good agreement between experiments and molecular simulations.

The experimental and simulated phase equilibria depicted in Figure 2 agree within the statistical uncertainties of the simulations. Furthermore, it can be seen from the enlarged part of this ternary plot that the simulations are also able to reproduce the vapor side mole fractions with a reasonable accuracy. At this temperature and pressure, the PR-EoS also provides a good prediction for the equilibrium concentrations.

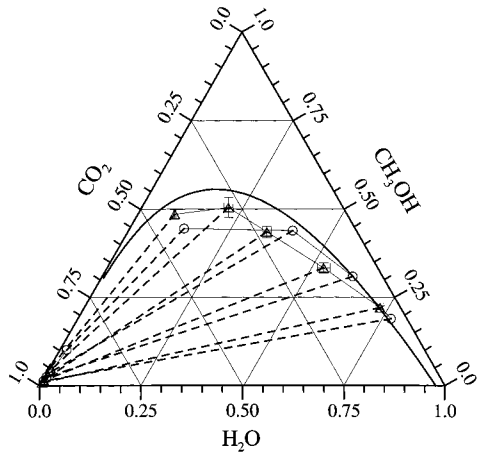

Figure 4. Liquid−liquid equilibrium mole fractions at 313.15 K and 12.0 MPa. ○, experimental results[2]; △, two-phase Gibbs ensemble simulations (error bars indicate statistical uncertainties). Coexisting state points are connected by dashed lines. The solid line denotes results from the PR-EoS[24] for the boundary of the two-phase region.

At the highest carbon dioxide concentration in the liquid phase, two of the simulation results are highlighted in Figure 2 by different symbols. The triangles denote the simulation results obtained by taking into account the long-range Coulomb interactions via Ewald sums; the square and the diamond mark the simulation results where the reaction field method was applied. In the case of the latter, the geometric mean combining rules were used whereas the Lorentz−Berthelot combining rules were employed in all other cases. The agreement between the data calculated by using different long-range corrections is good, while the difference appears to be greater between the simulation results obtained with different combining rules. However, considering the statistical uncertainties, these points can also be assumed to be practically indistinguishable (see also Table 1).

At 313.15 K and 10 MPa as well as at 12 MPa, the simulation results for the densities of the coexisting phases indicate liquid−liquid equilibrium. The overall accuracy of reproduction of the experiment by simulation is somewhat poorer at 12 MPa than at 10 MPa (cf. Figures 3 and 4). However, it is difficult to compare the quality of the results since the uncertainty of the experimental data is not known and the fluctuation in the less dense phase is relatively high at these pressures. Table 1 also illustrates the high statistical errors obtained at 10 MPa and at 12 MPa for the density of the less dense phase, which may be as large as 20%. Unfortunately, experimental data for the densities are not available.

Although the quality of the predictions for the liquid−liquid equilibrium obtained from the PR-EoS at 313.15 K seems to be less satisfactory at higher carbon dioxide concentrations and high pressures (cf. Figures 3 and 4), they have to be used as a reference for the simulation results at temperatures and pressures where no experimental data are available. Figure 5 shows such a comparison for several temperatures between 303 and 353 K and pressures between 2 and 8 MPa. The densities of the coexisting phases obtained from two-phase molecular simulations indicate a vapor−liquid equilibrium for the thermodynamic states illustrated. However, at 303.15 K and 7 MPa (cf. Figure 5a) a three-phase equilibrium is also expected (cf. Figure 1). The numerical data from Figure 5 are summarized in Table 2.

A detailed investigation of the phase equilibrium, especially of the pressure−density dependence of a mixture of a given composition, was performed at temperatures near the critical

TABLE 1: Properties of Coexisting Phases in Carbon Dioxide−Methanol−Water at 313.15 K from Two-Phase Gibbs Ensemble Simulations: Density (ρ), Residual Internal Energy (u), and Mole Fraction (x)[a]

p/MPa	ρ^L/(kg/m^3)	ρ^V/(kg/m^3)	u^L/(kJ/kg)	u^V/(kJ/kg)	$x^L_{CO_2}$	$x^L_{CH_3OH}$	$x^L_{H_2O}$	$x^V_{CO_2}$	$x^V_{CH_3OH}$	$x^V_{H_2O}$
7.0	873.9(47)	176.8(85)	−1291(42)	−50.3(26)	0.118(19)	0.441(10)	0.441(10)	0.994(2)	0.005(2)	0.001(1)
7.0	919.5(53)	178.6(56)	−1751(43)	−50.8(16)	0.038(11)	0.225(2)	0.737(9)	0.996(1)	0.003(1)	0.001(1)
7.0	891.2(47)	177.9(74)	−1507(36)	−50.9(26)	0.065(12)	0.361(5)	0.574(8)	0.994(1)	0.005(1)	0.001(1)
7.0	866.7(49)	177.5(63)	−1248(36)	−51.1(22)	0.120(16)	0.493(9)	0.387(7)	0.991(4)	0.007(2)	0.002(2)
7.0	853.8(65)	180.0(88)	−961(36)	−52.0(32)	0.244(24)	0.533(17)	0.223(7)	0.992(4)	0.007(3)	0.001(1)
7.0	844.3(55)	180.6(85)	−832(44)	−52.5(39)	0.310(35)	0.582(29)	0.108(6)	0.991(5)	0.008(5)	0.001(1)
7.0[b]	836(21)	178.3(42)	−836(47)	−51.7(15)	0.301(50)	0.590(42)	0.109(9)	0.991(1)	0.008(1)	0.001(1)
7.0[c]	844(19)	178.3(56)	−871(47)	−52.0(16)	0.276(49)	0.611(41)	0.113(8)	0.991(2)	0.008(2)	0.001(1)
10.0	923.7(53)	520(110)	−1738(25)	−136(30)	0.042(7)	0.222(3)	0.736(6)	0.985(1)	0.011(9)	0.004(4)
10.0	892.1(57)	560(110)	−1451(56)	−154(35)	0.088(21)	0.349(7)	0.563(15)	0.969(3)	0.023(18)	0.008(8)
10.0	874.5(53)	620(120)	−1205(33)	−180(34)	0.145(17)	0.473(11)	0.382(8)	0.945(3)	0.050(24)	0.005(4)
10.0	863.5(61)	510(120)	−826(35)	−129(30)	0.345(27)	0.462(19)	0.193(8)	0.987(10)	0.012(10)	0.001(1)
12.0	923.0(66)	667(59)	−1707(32)	−165(13)	0.051(9)	0.220(2)	0.729(7)	0.990(7)	0.008(5)	0.002(2)
12.0	898.6(76)	699(71)	−1337(61)	−174(18)	0.134(25)	0.333(9)	0.533(16)	0.984(8)	0.014(8)	0.002(2)
12.0	877.3(77)	677(78)	−1061(43)	−171(20)	0.222(24)	0.435(13)	0.343(11)	0.982(1)	0.016(12)	0.002(2)
12.0	864.7(76)	701(55)	−914(56)	−192(26)	0.281(39)	0.505(27)	0.214(11)	0.954(3)	0.042(25)	0.004(4)
12.0	863(12)	736(56)	−702(19)	−203(30)	0.424(17)	0.485(14)	0.091(3)	0.948(4)	0.050(35)	0.002(2)

[a] The liquid and vapor (or less dense liquid) phases are labeled by L and V, respectively. The numbers in parentheses represent the statistical uncertainties in the last digits (e.g., the notation 873.9(47) means 873.9 ± 4.7). [b] Reaction field method and Lorentz−Berthelot combining rules. [c] Reaction field method and geometric mean combining rules.

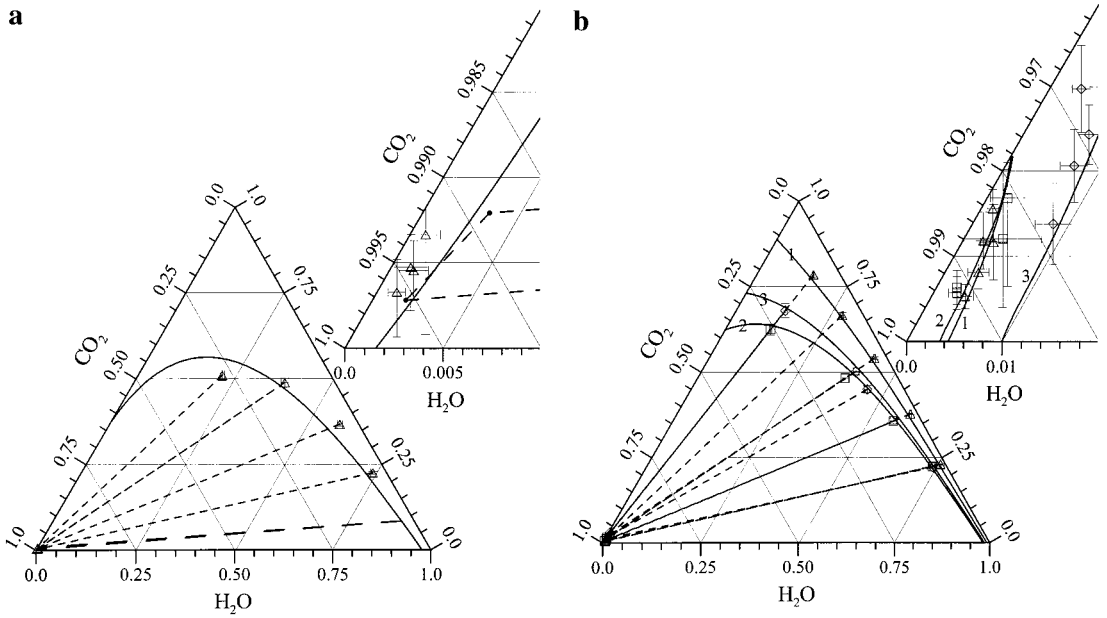

Figure 5. (a) Phase equilibrium mole fractions at 303.15 K and 7.0 MPa. △, two-phase Gibbs ensemble simulations (error bars indicate statistical uncertainties). Coexisting state points are connected by dashed lines. The solid line denotes results from the PR-EoS[24] for the boundary of the two-phase region. The long-dashed line indicates the three-phase region. (b) Phase equilibrium mole fractions from two-phase Gibbs ensemble simulations (symbols; error bars indicate statistical uncertainties) and from the PR-EoS[24] (numbered solid lines indicate the boundary of the two-phase region): △ and (1) at 313.15 K, 2.0 MPa; □ and (2) at 323.15 K, 7.0 MPa; ◇ and (3) at 353.15 K, 8.0 MPa. Coexisting state points are connected by dashed lines.

temperature of carbon dioxide. For two temperatures, one (298.15 K) slightly lower and one (308.15 K) slightly higher than the critical temperature of carbon dioxide (304.2 K), two-phase *NpT*-GEMC simulations of a mixture with a fixed overall composition were carried out at pressures from 5 to 11 MPa. For the state points examined, the simulation always produced very similar results for the composition of the high-density liquid phase (see Table 3). Figure 6 shows the results for the low-density phase. At 298.15 K a jump in the density is observed when the pressure is increased. At 308.15 K (and also at 313.15 K) the density of that phase no longer reveals such a jump but a continuous transition to a denser state. The jump indicates a transition from a vapor−liquid to a liquid−liquid equilibrium. The pressure range of this transition corresponds to (or is somewhat higher than) the three-phase equilibrium range shown in Figure 1. At 308.15 K the simulation results in that region bear large statistical errors, while at 298.15 K no results were obtained in the density range between 300 and 700 kg/m^3. The 313.15 K isotherm shown in Figure 6 was constructed by selecting data (with nearly identical composition of the high-density liquid phase) from Table 1 for three pressures.

Initially, the multiphase GEMC method was utilized for the screening of regions where three-phase coexistence is observed experimentally. The method allows for the investigation of more than two coexisting phases in one simulation by setting up as many simulation boxes as phases that are expected to be present. For the carbon dioxide−methanol−water system in three-phase equilibrium, the "three-boxes" simulations were performed at fixed temperature, and in most cases the pressure was also fixed. Starting with boxes with identical composition and density, the

TABLE 2: Properties of Coexisting Phases in Carbon Dioxide−Methanol−Water from Two-Phase Gibbs Ensemble Simulations: Density (ρ) and Mole Fraction (x)[a]

T/K	p/MPa	ρ^L/(kg/m^3)	ρ^V/(kg/m^3)	$x^L_{CO_2}$	$x^L_{CH_3OH}$	$x^L_{H_2O}$	$x^V_{CO_2}$	$x^V_{CH_3OH}$	$x^V_{H_2O}$
303.15	7.0	933(8)	250(120)	0.035(7)	0.225(2)	0.740(5)	0.996(3)	0.003(3)	0.001(1)
303.15	7.0	908(7)	216(18)	0.048(11)	0.368(4)	0.584(7)	0.994(2)	0.005(2)	0.001(1)
303.15	7.0	882(6)	209(15)	0.129(21)	0.488(12)	0.383(9)	0.994(3)	0.005(3)	0.001(1)
303.15	7.0	874(5)	205(15)	0.277(21)	0.510(15)	0.213(6)	0.992(7)	0.007(7)	0.001(1)
313.15	2.0	904(6)	36.3(2)	0.014(4)	0.230(1)	0.756(3)	0.991(2)	0.005(2)	0.004(1)
313.15	2.0	879(5)	36.3(2)	0.020(4)	0.378(2)	0.602(3)	0.988(2)	0.008(2)	0.004(1)
313.15	2.0	848(6)	36.3(2)	0.034(6)	0.541(3)	0.425(3)	0.985(5)	0.012(5)	0.003(1)
313.15	2.0	824(5)	36.4(2)	0.055(10)	0.666(7)	0.279(4)	0.986(4)	0.012(4)	0.002(1)
313.15	2.0	809(5)	36.4(2)	0.070(11)	0.784(9)	0.146(2)	0.983(5)	0.016(4)	0.001(1)
323.15	7.0	907(8)	161(4)	0.038(11)	0.224(2)	0.738(9)	0.992(2)	0.006(2)	0.002(1)
323.15	7.0	876(4)	157(3)	0.075(14)	0.357(5)	0.568(8)	0.992(3)	0.006(2)	0.002(1)
323.15	7.0	848(6)	159(4)	0.139(19)	0.482(10)	0.379(8)	0.984(12)	0.012(8)	0.004(4)
323.15	7.0	820(6)	162(7)	0.260(20)	0.624(17)	0.116(3)	0.981(13)	0.017(11)	0.002(2)
353.15	8.0	816(7)	154(5)	0.099(16)	0.449(8)	0.452(8)	0.972(5)	0.021(5)	0.007(1)
353.15	8.0	872(7)	153(3)	0.038(9)	0.222(2)	0.740(8)	0.978(6)	0.014(5)	0.008(2)
353.15	8.0	810(7)	154(3)	0.101(15)	0.502(8)	0.397(7)	0.969(4)	0.024(4)	0.007(1)
353.15	8.0	771(8)	154(3)	0.194(26)	0.679(22)	0.127(4)	0.967(6)	0.030(6)	0.003(1)

[a] The liquid and vapor (or less dense liquid) phases are labeled by L and V, respectively. The numbers in parentheses represent the statistical uncertainties in the last digits (e.g., the notation 933(8) means 933 ± 8).

TABLE 3: Properties of Coexisting Phases in Carbon Dioxide−Methanol−Water from Two-Phase Gibbs Ensemble Simulations: Density (ρ) and Mole Fraction (x)[a]

T/K	p/MPa	ρ^L/(kg/m^3)	ρ^V/(kg/m^3)	$x^L_{CO_2}$	$x^L_{CH_3OH}$	$x^L_{H_2O}$	$x^V_{CO_2}$	$x^V_{CH_3OH}$	$x^V_{H_2O}$
308.15	6.0	872(13)	148(3)	0.129(20)	0.491(11)	0.380(9)	0.995(2)	0.004(2)	0.001(1)
308.15	7.0	875(18)	188(10)	0.134(30)	0.488(16)	0.378(14)	0.993(3)	0.006(3)	0.001(1)
308.15	7.8	881(17)	241(18)	0.142(32)	0.483(18)	0.375(14)	0.993(2)	0.006(2)	0.001(1)
308.15	8.2	881(20)	294(45)	0.171(37)	0.465(20)	0.364(17)	0.988(7)	0.011(7)	0.001(1)
308.15	8.6	882(14)	391(102)	0.178(25)	0.462(14)	0.360(11)	0.990(4)	0.008(3)	0.001(1)
308.15	9.0	883(18)	535(121)	0.200(30)	0.449(17)	0.351(14)	0.986(8)	0.012(7)	0.002(2)
308.15	10.0	885(25)	705(52)	0.173(37)	0.456(17)	0.371(22)	0.958(29)	0.035(22)	0.007(7)
308.15	11.0	887(17)	734(30)	0.182(30)	0.452(17)	0.366(14)	0.965(17)	0.030(13)	0.004(4)
298.15	5.0	883(12)	119(4)	0.106(18)	0.505(10)	0.389(8)	0.996(2)	0.003(2)	0.001(1)
298.15	6.0	889(14)	162(7)	0.138(26)	0.487(15)	0.375(11)	0.996(1)	0.003(1)	0.001(1)
298.15	7.0	894(12)	244(24)	0.143(22)	0.483(12)	0.374(10)	0.995(2)	0.004(1)	0.001(1)
298.15	7.0	895(11)	766(38)	0.127(16)	0.467(13)	0.406(15)	0.930(24)	0.061(21)	0.009(4)
298.15	8.0	897(13)	780(40)	0.173(24)	0.450(18)	0.377(10)	0.934(33)	0.052(24)	0.014(11)
298.15	9.0	897(21)	785(28)	0.173(36)	0.460(21)	0.367(16)	0.976(11)	0.021(10)	0.002(2)

[a] The liquid and vapor (or less dense liquid) phases are labeled by L and V, respectively. The numbers in parentheses represent the statistical uncertainties in the last digits (e.g., the notation 872(13) means 872 ± 1.3).

boxes tended toward three distinct phases at slightly higher pressures than those expected from the experimental data. However, the convergence of these simulations was very slow and some box identity switches occurred during the simulations. In all cases, two of the three peaks of the determined density or composition probability functions were not clearly separated and/or their shapes or positions were uncertain. Consequently, neither accurate density nor concentration results for the coexisting phases could be determined from ensemble averages at the temperatures where experimental three-phase coexistence data are available. This is probably due to the fact that all state points, which were found within the three-phase area, lie close to a critical (lower or upper) endpoint line and only low-energy barriers separate the three phases. Nevertheless, at 298.15 K a constant-volume GEMC (i.e., *NVT*-GEMC) yielded stable three-phase equilibrium data at the average pressure $p = 6.9 \pm 0.3$ MPa resulting in densities $\rho^{L_1} = 894 \pm 13$ kg/m^3, $\rho^{L_2} = 733 \pm 43$ kg/m^3, and $\rho^V = 265 \pm 41$ kg/m^3. The mole fraction results are in qualitative agreement with the experimental data measured at somewhat higher temperatures (see Table 4). Simulations carried out at temperatures lower than 298.15 K encountered difficulties with particle transfers, despite the sophisticated particle exchange methods[14−18] used.

As an alternative, two-phase semi-grand canonical GEMC simulations were performed at the temperature of one of the experimental three-phase points to find evidence of the three-phase coexistence of the model system without calculating direct ensemble averages. Under the consideration of the results of

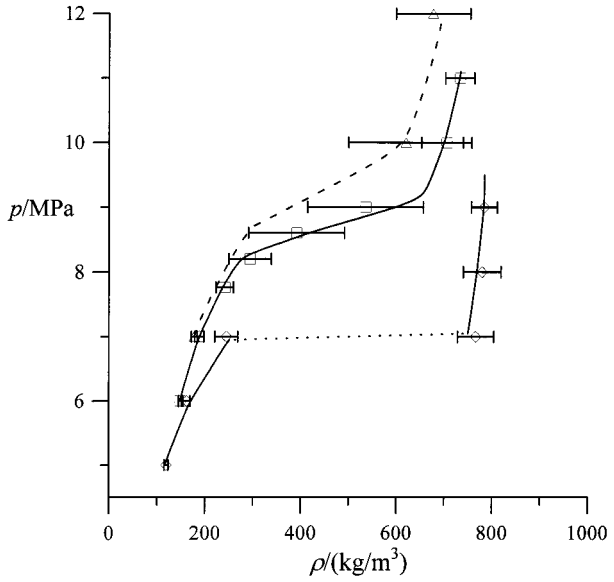

Figure 6. Density of the less dense phase in equilibrium with a (denser) liquid phase from two-phase Gibbs ensemble simulations at 298.15 (◇), 308.15 (□), and 313.15 K (△). Error bars indicate the statistical uncertainties.

TABLE 4: Mole Fraction (x) Results for Three-Phase Coexistence in Carbon Dioxide−Methanol−Water[a]

T/K	p/MPa	$x^{L_1}_{CO_2}$	$x^{L_1}_{CH_3OH}$	$x^{L_2}_{CO_2}$	$x^{L_2}_{CH_3OH}$	$x^{V}_{CO_2}$	$x^{V}_{CH_3OH}$
298.15	6.9(3)	0.125(21)	0.477(13)	0.962(17)	0.035(15)	0.990(8)	0.008(6)
305.15[b]	7.20	0.396	0.485	0.895	0.091	0.975	0.022
305.15[b]	7.37	0.101	0.367	0.907	0.048	0.989	0.009
305.15[b]	7.50	0.031	0.162	0.917	0.020	0.991	0.005
308.15[b]	7.65	0.468	0.448	0.903	0.084	0.988	0.011
308.15[b]	7.76	0.180	0.468	0.930	0.047	0.985	0.013
308.15	8.60	∼0.17	∼0.45	≥0.995	<0.005	≥0.995	<0.005
311.15[b]	8.10	0.416	0.475	0.917	0.072	0.983	0.016

[a] The liquid and vapor phases are labeled by L_1, L_2, and V. The numbers in parentheses represent the statistical uncertainties in the last digits (e.g., the notation 0.125(21) means 0.125 ± 0.021). [b] Experimental result.[2]

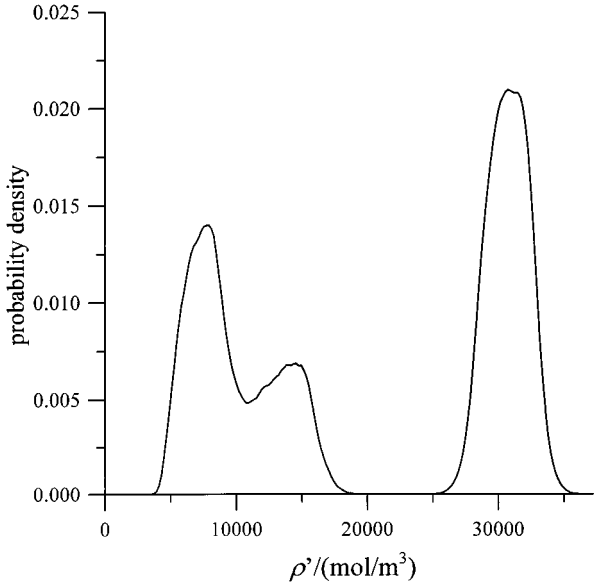

Figure 7. Number density (ρ') distribution obtained from two-phase semi-grand canonical GEMC simulation at 308.15 K and 8.6 MPa.

the multiphase GEMC simulations, the semi-grand canonical simulations were carried out with the intention of observing a high-density subsystem (in one of the boxes) and a coexisting subsystem (in the other box) fluctuating between a vaporlike and a liquidlike density value. The simulations were designed for frequent transitions of the latter subsystem between two low-density bulk phases to obtain a characteristic trimodal density distribution for the whole system. This was achieved by adjusting the pressure and the difference between the chemical potentials of methanol and water for the whole system. As the semi-grand canonical step implies a preset chemical potential difference, the overall composition is not fixed and the transition between two phases in a single simulation box becomes easier. In brief, this method allows better sampling efficiency for a finite system near (or at) a critical point. Figure 7 shows the number density (ρ') distribution obtained from a semi-grand canonical GEMC simulation at 308.15 K and 8.6 MPa. The three distinct peaks in Figure 7 indicate that three phases, a high-density liquid and two less dense phases, are sampled. The average density of the first liquid phase amounts to approximately 890 kg/m^3 (when using the mole fractions from Table 4, which are extracted from the peak positions of the mole fraction distributions; this distribution function is not presented here). The peaks representing the vapor and the second liquid phase are not completely separated, and the mole fractions obtained for these phases are not distinguishable within the scattering of the simulation results. The estimated densities of the two phases are about 340 and 650 kg/m^3. A qualitatively similar behavior was found at this thermodynamic state (308.15 K and 8.6 MPa) when the intermolecular potential of water was described by the TIP4P model (instead of the SPC model). Moreover, the appearance of three distinct peaks does not depend on whether the Lorentz−Berthelot or the geometric mean combining rules are used. Accordingly, this result provides stronger evidence of three-phase coexistence than the pressure dependence curves shown in Figure 6. However, a strict comparison of the calculated mole fraction data with the experimental results is not feasible as the composition of the dense liquid phase is too sensitive to small variations in the pressure (cf. the experimental mole fraction data in Table 4). Furthermore, because of overlapping peaks, the question of whether the state point examined lies within the three-phase region or just in the immediate vicinity of a critical endpoint line still remains unanswered.

4. Summary and Conclusions

The high-pressure phase equilibrium of the ternary model system carbon dioxide−methanol−water was studied by molecular simulation at temperatures near the critical temperature of carbon dioxide. The system was modeled by intermolecular potentials, which were described by a combination of Lennard-Jones and Coulomb sites. The pure component pair potentials were adopted from the literature. Common combining rules without any adjustable parameters were employed to model the cross interactions. Vapor−liquid as well as liquid−liquid equilibria were observed in the simulations. The simulation results for the density of the coexisting phases could be used to distinguish vapor−liquidlike and liquid−liquidlike two-phase equilibria. (It should be noted that the experimental data for the carbon dioxide−methanol−water system reveal only a very small difference in the compositions of the less dense coexisting phases in liquid−liquid−vapor equilibrium.) Furthermore, the occurrence of three-phase equilibrium could be observed despite the very narrow three-phase region in this system. At a temperature slightly lower than the critical temperature of carbon dioxide, the multiphase GEMC simulation provided reliable results for three-phase coexistence. At higher temperatures, where experimental three-phase equilibrium data are available, multiphase behavior was found at a pressure somewhat above the experimental data. Thus, qualitative and also in some cases quantitative agreement was found between molecular simulation and experiments.

Acknowledgment. The authors give due thanks to the Regionales Hochschulrechenzentrum Kaiserslautern (RHRK) for providing computing time on their supercomputers. The authors furthermore thank Dipl.-Ing. Georg Sieder for supplying results from the PR-EoS of Adrian et al.[24] T.K. gratefully acknowledges a scholarship from the Deutscher Akademischer Austauschdienst (DAAD).

References and Notes

(1) Efremova, G. D.; Shvarts, A. V. *Russ. J. Phys. Chem.* **1966**, *40*, 486.
(2) Yoon, Y.-H.; Chun, M.-K.; Hong, W.-H.; Lee, H. *Fluid Phase Equilib.* **1993**, *32*, 2881.
(3) Panagiotopoulos, A. Z. *Mol. Phys.* **1987**, *61*, 813.
(4) Panagiotopoulos, A. Z.; Quirke, N.; Stapleton, M.; Tildesley, D. J. *Mol. Phys.* **1987**, *61*, 813.
(5) de Miguel, E.; Martín del Río, E.; Telo da Gama, M. M. *J. Chem. Phys.* **1995**, *103*, 6188.
(6) Escobedo, F. A. *J. Chem. Phys.* **2001**, *115*, 5642.
(7) Canongia Lopes, J. N.; Tildesley, D. J. *Mol. Phys.* **1997**, *92*, 187.
(8) Lísal, M.; Smith, W. R.; Nezbeda, I. *Fluid Phase Equilib.* **2001**, *181*, 127. The reports on molecular simulation of the high-pressure vapor−liquid equilibrium for real mixtures are also scanty in the literature. One of the first simulation results of such two-phase equilibrium was obtained for the ternary mixture methane−ethane−carbon dioxide (Vrabec, J.; Fischer, J. *AIChE J.* **1997**, *43*, 212.) by using the *NpT*+test particle method.
(9) Lísal, M.; Smith, W. R.; Nezbeda, I. *J. Phys. Chem. B* **1999**, *103*, 10496.
(10) Harris, J. G.; Yung, K. H. *J. Phys. Chem.* **1995**, *99*, 12021.
(11) van Leeuwen, M. E.; Smit, B. *J. Phys. Chem.* **1995**, *99*, 1831.
(12) Berendsen, H. J. C.; Postma, J. P. M.; van Gunsteren, W. F.; Hermans, J. In *Intermolecular Forces*; Pullmann, B., Ed.; Reidel: Dordrecht, 1981; p 331.
(13) Jorgensen, W. L.; Chandrasekhar, J.; Madura, J. D.; Impey, R. W.; Klein, M. L. *J. Chem. Phys.* **1983**, *79*, 926.
(14) Smit, B.; Karaborni, S.; Siepmann, J. I. *J. Chem. Phys.* **1995**, *102*, 2126.
(15) Cracknell, R. F.; Nicholson, D.; Parsonage, N. G.; Evans, H. *Mol. Phys.* **1990**, *71*, 931.
(16) Loyens, L. D. J. C.; Smit, B.; Esselink, K. *Mol. Phys.* **1995**, *86*, 171.
(17) Vorholz, J.; Harismiadis, V. I.; Rumpf, B.; Panagiotopoulos, A. Z.; Maurer, G. *Fluid Phase Equilib.* **2000**, *170*, 203.
(18) Panagiotopoulos, A. Z. *Int. J. Thermophys.* **1989**, *10*, 447.
(19) Escobedo, F. A. *J. Chem. Phys.* **2000**, *113*, 8444.
(20) Allen, M. P.; Tildesley, D. J. *Computer Simulation of Liquids*; Clarendon: Oxford, 1987.
(21) Neumann, M. *J. Chem. Phys.* **1985**, *82*, 5663.
(22) Theodorou, D. N.; Suter, U. W. *J. Chem. Phys.* **1985**, *82*, 955.
(23) de Leeuw, S. W.; Perram, J. W.; Smith, E. R. *Proc. R. Soc. London, Ser. A* **1980**, *A373*, 27.
(24) Adrian, T.; Wendland, M.; Hasse, H.; Maurer, G. *J. Supercrit. Fluids* **1998**, *12*, 185.